

## SCALE OF RESISTANCE OF BUILDINGS TO MINING INFLUENCES – APPLICABILITY ASSESMENT THROUGH A CASE STUDY

Katarzyna NOWAK <sup>a\*</sup>, Piotr STRZAŁKOWSKI <sup>b</sup>, Leszek SZOJDA <sup>c</sup>

<sup>a</sup> MSc Eng.; The Silesian University of Technology, Faculty of Civil Engineering, ul. Akademicka 5, 44-100 Gliwice, Poland

\* Corresponding author. E-mail address: [Katarzyna.Nowak@polsl.pl](mailto:Katarzyna.Nowak@polsl.pl)

<sup>b</sup> Prof.; The Silesian University of Technology, Faculty of Mining, Safety Engineering and Industrial Automation, ul. Akademicka 2, 44-100 Gliwice, Poland

<sup>c</sup> Prof.; The Silesian University of Technology, Faculty of Civil Engineering, ul. Akademicka 5, 44-100 Gliwice, Poland

Received: 31.12.2021; Revised: 21.08.2023; Accepted: 25.08.2023

### Abstract

This paper presents a case study of the impact of continuous deformations and rock mass tremors on a single-family building, typical of Upper Silesia. In the areas subjected to the influence of ground deformation, a point method for assessing the resistance of buildings to these influences has been developed by the Central Mining Institute. As part of this method, the geometric parameters, structure, materials and technical condition of the facility, as well as the ground on which the building is located, are taken into account. A case study considers a building being simultaneously subjected to continuous deformations and mining tremors. The object's resistance is assessed according to the point method and its technical condition is assessed after revealing the influence of ground deformation. This is used to assess the validity of the point method for the building. On the basis of the analyses of the state of deformation and the impact of tremors, conclusions are drawn regarding the need to make changes to the scale used to assess the category of resistance of buildings to the effects of continuous deformation.

**Keywords:** Continuous deformation; Ground deformation; Masonry structures; Mining damage; Mining impact on environment; Point method; Residential building.

## 1. INTRODUCTION

The underground mining of deposits causes certain negative consequences for the natural environment, regardless of the geological and mining conditions; these include natural objects and urban developments with infrastructure. The environmental impact of mining using underground and opencast methods is presented in the work by [1, 2, 24]. In the case of opencast and underground mining, among the negative effects on the environment, there are problems related to the storage of waste, changing water relations, and deformation of the rock mass. Waste disposal in heaps is a threat to the environment due to the impact of harm-

ful chemical compounds on groundwater, reservoirs and water courses [14, 22]. Research is currently being undertaken to consider using post-mining waste for economic purposes, a good example of which is the use of waste from iron ore enrichment as a raw material for the production of roof tiles [4].

Apart from the occurrence of floodplain areas, as a result of depressions in the areas above underground mines [2], there is also an impact of opencast mining works on groundwater [29]. For obvious reasons, changes in water conditions should be carefully considered when it comes to their impact on buildings [9].

Surface deformations are the most socially burdensome

form of impact of underground mining on the environment. These deformations are divided into continuous (always accompanying the underground mining of deposits) and discontinuous (mainly sinkholes occurring at the surface or linear features, e.g. terrain steps). Due to the frequency of occurrence and the effects they cause, continuous deformations, in the form of subsidence troughs and their derivatives, are of particular interest. Therefore, a number of deformation forecasting methods have been developed, of which the Knothe model [10], also popular in China [31], is very often used. The issue is even more relevant when, as is the case in Poland [2] and in China [18], there is an increase in extraction under areas with a built environment and natural objects, including reservoirs and water courses. Abundant literature on the subject provides us with knowledge about many cases of the destructive impact of mining operations on such objects [5, 11, 16, 17, 30]. A separate issue is the combined effects of continuous deformations and rock tremors, as noted by Strzałkowski [23].

This article presents a case study of the impact of continuous deformation and rock mass tremors on a single-family building, which is typical of those in Upper Silesia. On the basis of the state analysis of deformation and the impact of tremors, conclusions are drawn regarding the need to make changes to the scale used to assess the category of resistance of buildings to the effects of continuous deformation.

## 2. MATERIALS AND METHODS

Hard coal deposits in Upper Silesia are located in highly urbanised areas. The underground exploitation of deposits causes subsidence of the land surface as a result of the post-mining voids being filled with material collapsing from the layers above. Objects located on the ground surface are subjected to additional influences and, if they are not properly protected against these influences, they can suffer significant damage. Damage to structural elements, or the deflection of the entire structure from the vertical, sometimes causes significant defects in the finishing elements and this, in turn, causes the need for additional renovations and repairs that significantly increase maintenance costs. Pursuant to the applicable “Geological and Mining Law” [28], mining entrepreneurs are obliged to repair the damage caused by exploitation effects, which are included in the raw material exploitation costs. In order to determine the profitability of exploitation, it is necessary to determine how large deformations of the ground are able

to accommodate objects located on the ground surface. The magnitude of the impact of continuous ground deformation on building structures is determined in the USCB (Upper Silesian Coal Basin) using the Knothe theory [10]. This well-known theory is used in the analysis carried out in this paper but is not explained here. According to the existing recommendations [7], in designed objects it is possible to define the size of structural elements protecting against the occurrence of additional internal forces caused by ground deformations. In older buildings that have not been adapted to transfer mining deformations, a detailed analysis of the structure is often necessary [3, 20, 25] and, sometimes, drastic steps have to be taken to protect the buildings against excessive subsoil impact [8]. Discontinuous deformations of the ground, which have a much greater impact on buildings, require provisions in the structure before these deformations occur at the design stage, or significant structural modifications in already existing buildings [26].

Detailed static and strength analysis of the objects is not possible for the large number of objects which must be assessed in a short period of time before starting the exploitation of the coal seams. For this reason, in the areas subjected to the influences of ground deformations, a point method for assessing the resistance of objects to the effects of ground deformation was developed by the Central Mining Institute [12]. As part of this method, the geometric parameters, structures, materials and technical conditions of the facility, as well as the ground on which the building is located, are taken into account.

The description of the use of the modified point method was presented, *inter alia*, in [13]. However, it should be noted that the scope of applicability of this method was limited to residential buildings with typical structures and foundations. It also applies to continuous deformations of the subsoil, the extent, intensity and duration of which resembles mild trough subsidence and develops in a static manner over months and years. It cannot be used in relation to discontinuous deformations and it does not include the effects of tremors of the mining ground.

The analysis of a case study, presented below, considers an object that was simultaneously subjected to continuous deformation and mining tremors. The object's resistance was assessed according to the point method and its technical condition was assessed after revealing the influence of ground deformation. This was used to assess the validity of the point method used for this object.

### 3. CASE STUDY

#### 3.1. Mining conditions

##### 3.1.1. Lithology and stratigraphy

The orogen in the area under consideration comprises overburden layers and productive carbon (see Fig. 1). The overburden is made of Quaternary Formations consisting of yellow sands, sandy grey clays, and grey and yellow chanterelles. The thickness of these layers at the building locations ranges from 20–40 m. The productive carbon is made of Orzeskie (300 groups), Rudzkie (400 groups) and Saddle layers (500 groups). In the period under consideration, mining was carried out in the Orzeskie and Saddle Beds, which have high carbon content.

##### 3.1.2. Tectonics

Fault V runs through the area under consideration. This fault has dumped layers in a south-east direction, to a height of approximately 70 m. The outcrop of the fault on the carboniferous ceiling is located 75 m from the property. The ground deformation caused by the fault does not affect the building, but its location causes a disturbance in the propagation of shock in the ground layer and can negatively affect the building.

##### 3.1.3 Mining exploitation performed

Intensive mining operations were carried out in the vicinity of the facility. This exploitation was performed on the following coal seams:

- 402/1 in the years 1970–72, with a hydraulic backfill and a fall-of-roof at a depth of approximately 250 m, at the shortest distance from the facility (approximately 150 m).
- 405 in the years 1975–84, with a hydraulic backfill and a fall-of-roof at a depth of approximately 400 m, at the shortest distance from the facility (approximately 20 m).
- 409 in the years 1977–84, with a fall-of-roof at a depth of approximately 400 m, at the shortest distance from the facility (approximately 10 m).
- 410 in the years 1980–88, with the fall-of-roof directly below the facility, at a depth of approximately 480 m.
- 411 in the years 1982–92, with a fall-of-roof at a depth of approximately 500 m, at the shortest distance from the facility (approximately 500 m).
- 504 in the years 1974–75, with a fall-of-roof at

a depth of approximately 730 m and at a distance of 150–200 m.

- 506 in the years 1988–92, with the fall-of-roof at a depth of approximately 780–850 m, also directly below the facility.
- 507 in the years 1984–97, with a fall-of-roof at a depth of approximately 820–880 m, at a distance of 150–200 m.
- 510 layer I in the years 1985–88, with a fall-of-roof at a depth of approximately 800 m, at a distance from the facility of approximately 210 m.

The last exploitation was carried out in the area of the building in 2009. When summarising the influence of exploitation on the surface, it was decided to follow the view of Knothe [10], who proposed grouping the deformations into 10-year periods.

Table 1 presents the basic geological and mining condition data from the mining conducted in the period 2000–2009.

The location of the exploitation presented in Table 1, in relation to the object, is shown in Fig. 1.

The table shows the system of exploitation: *zd* – fall-of-roof with caulk, *z* – fall-of roof, *ph* – hydraulic filling.

##### 3.1.4. The impact of the exploitation on the building in light of the calculation results

The following parameter values were adopted for the calculations [10]:

- Size of settlement in relation to the thickness of the operated seam: for operation with fall-of-roof  $a = 0.8$ ; for operation with caulk  $a = 0.6$
- Tangent of the main influence range angle  $\tan \beta = 2.0$
- Coefficient of proportionality of horizontal displacements to slopes  $B = 0.32$
- Service edge  $d = 0$
- The correction for the inclination (slope) of the coal seam –  $d_u$ , was determined from Eq. (1):

$$d_u = (H - h) \tan(n \alpha) \quad (1)$$

where:

$H$  – depth of the exploitation,

$h$  – thickness of the exploitation,

$\alpha$  – dipping angle,

$n$  – a coefficient in the range  $\langle 0.2; 0.7 \rangle$ ,  $n = 0.7$  was assumed

**Table 1.**  
**Basic information on geological and mining conditions of the exploitation**

Coal seam	Wall/parcel	Beginning of expl.	End of expl.	Coal seam thick. [m]	Dipp. ang. [deg]	Dep. [m]	Dist. [km]	Dir.	Ang. [deg]	a	System
4131	sc_5	01-10-2003	30-06-2004	1.8	5	640	0.30	SW	65	0.60	zd
4131	sc_6	01-07-2003	31-03-2004	1.8	5	640	0.38	SW	59	0.60	zd
4132	sc_1	01-07-1999	10-09-2000	2.4	5	610	0.55	W	48	0.60	zd
4132	sc_2	15-12-2000	30-09-2002	2.4	5	610	0.25	W	68	0.60	zd
416	sc_10	01-10-2003	01-06-2004	1.8	5	685	0.44	W	57	0.80	z
416	sc_8	20-03-2000	21-01-2002	1.8	5	625	0.03	NW	87	0.80	z
416	sc_9	01-07-2001	18-04-2003	2	5	655	0.00	Bezp	90	0.80	z
502	18a	01-09-2007	31-03-2008	3	5	720	0.33	NE	65	0.25	ph
502	18b	01-04-2008	01-09-2008	2.5	5	700	0.65	NE	47	0.80	z
502	sc_17a	01-04-2006	31-12-2006	3	5	720	0.38	N	62	0.25	ph
502	sc_17b	01-01-2007	01-04-2007	2.5	5	700	0.66	N	47	0.80	z
502	sc_19	01-12-2008	03-08-2009	3	5	690	0.43	NE	58	0.25	ph
5102	sc_6	01-10-2000	01-08-2001	2	5	790	0.27	NE	71	0.60	zd
5102	sc_7	01-12-2001	01-10-2002	2	5	795	0.26	NE	72	0.60	zd
5102	sc_8	01-05-2002	31-07-2003	2	5	800	0.36	N	66	0.60	zd
5103	sc_7	01-06-2004	25-03-2005	2	5	800	0.33	NE	68	0.60	zd
5103	sc_8	01-01-2005	01-08-2005	2	5	800	0.41	N	63	0.60	zd

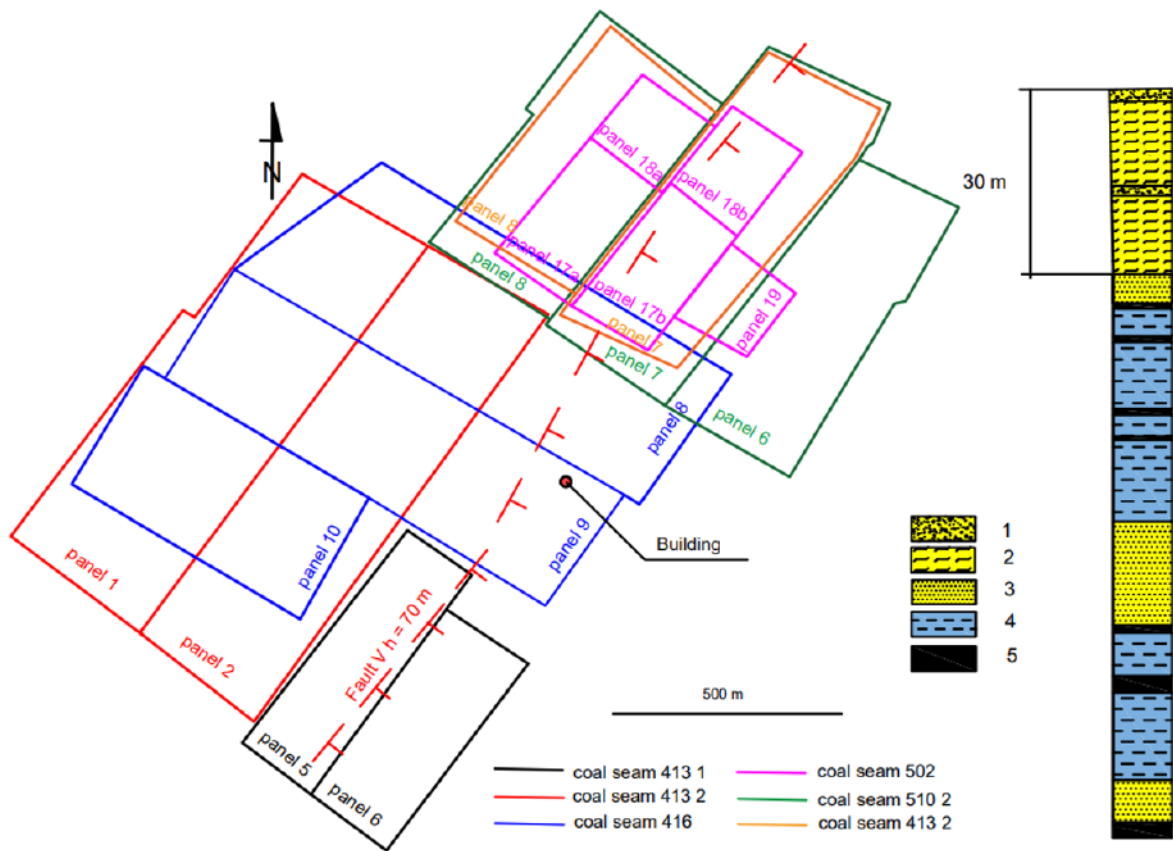


**Figure 1.**  
**Diagram of the location of the building in relation to selected walls and the lithological profile of the rock mass; 1 – sands, 2 – clays, 3 – sandstone, 4 – shale, 5 – coal**

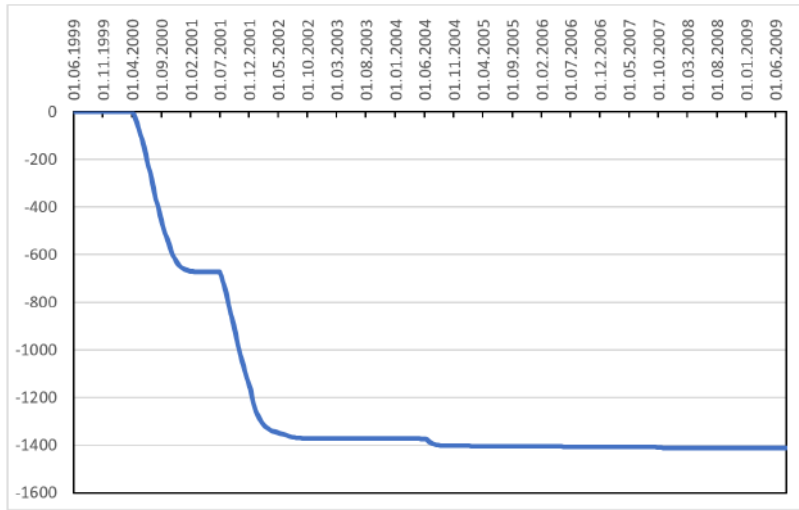


**Figure 2.**  
Graph of the increased subsidence calculated in relation to time according to Knothe's theory

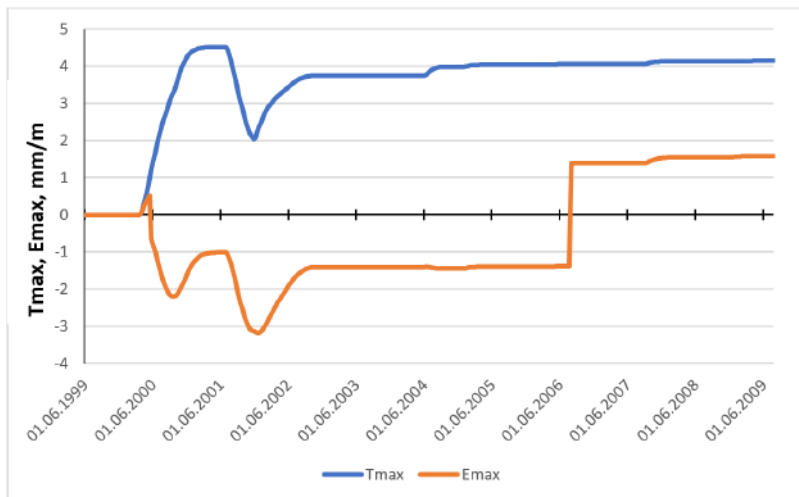


**Figure 3.**  
Graph of the calculated maximum slope ( $T_{max}$ ) and maximum horizontal strain ( $E_{max}$ ) in relation to time according to Knothe's theory

The following deformation indicators were calculated:

- $w$  – subsidence, mm
- $T_{max}$  – maximum slope, mm/m
- $E_{max}$  – maximum horizontal strain, mm/m

The calculations were carried out using the DEFK-Win program developed by Ścigała [27]. The progress of exploitation fronts was simulated with the assumption of immediate disclosure of influences. Fig. 2 shows the function graph of the subsidence and Fig. 3 shows the maximum slope and the maximum horizontal strain.

### 3.1.5. The impact of rock mass tremors on the object

The maximum values of the vibration acceleration component were calculated using Mutke's equation in [15]:

$$PGA = [1.33 \cdot 10^{-3} \cdot (\log E)^{2.66-0.089}] \cdot [1.53 \cdot R^{0.155} \cdot e^{-0.65 \cdot R} + 0.014] \quad (2)$$

The maximum amplitude of the horizontal component of the vibration velocity was calculated from Eq. (3):

$$PGV = [1.48 \cdot 10^{-3} \cdot (\log E)^{1.23-0.011}] \cdot [1.55 \cdot R^{0.135} \cdot e^{-0.77 \cdot R} + 0.04] \quad (3)$$

where:

$PGA$  – maximum amplitude of the horizontal

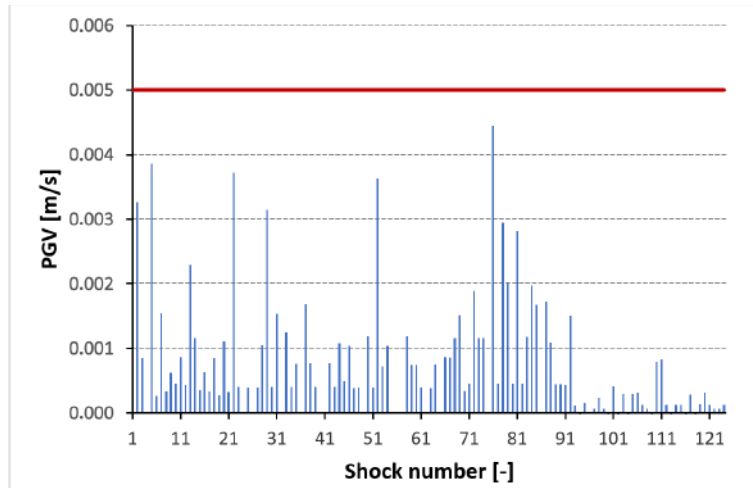


Figure 4.  
Calculated PGV values at the property site according to Eq. (3)

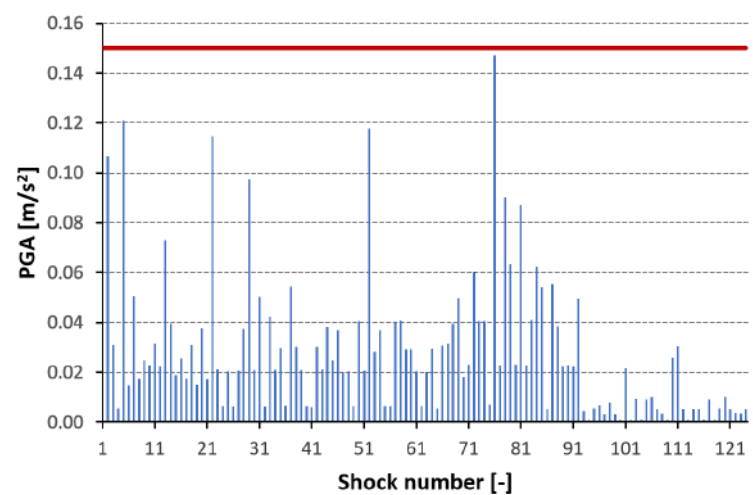


Figure 5.  
Calculated PGA values at the property site according to Eq. (2)

component of vibration acceleration,  $\text{m/s}^2$

$PGV$  – maximum amplitude of the horizontal component of the vibration velocity,  $\text{m/s}$

$$R = \sqrt{D^2 + 0.5^2} \quad (4)$$

$D$  – epicentral distance,  $\text{km}$

$E$  – shock energy (*The values of the shock energy  $E$  are assumed on the basis of the results of measurements carried out in mine seismic stations*),  $\text{J}$

Eq. (2) is correct for earthquakes with a seismic energy of  $1.0 \cdot 10^5 \leq E \leq 5.0 \cdot 10^8 \text{ J}$ .

Eq. (3) is correct for energy up to  $2 \cdot 10^9 \text{ J}$ .

These values correspond to carboniferous rocks. To get the value corresponding to the area of interest, the results obtained from Eqs. (2) and (3) should be multiplied by the (so-called) amplification factor, the

value of which would be  $k = 1.5$ , from the map of amplification factor values.

Based on Eqs. (2) and (3), the  $PGA$  and  $PGV$  values were calculated for all shocks from 2018 at the site of the building's foundation. The calculation results are shown in Figs. 4 and 5.

In both figures, a brown horizontal line marks the border of the 0 and I intensity degree. This boundary separates the degrees 0 and I, regardless of the duration of the intense phase of vibrations. Figs 4 and 5 show that all of the shocks shown can be classified according to  $PGV$  and  $PGA$  values at a 0 degree. Thus, according to the results of the calculations, the shocks should have no effect on the building.

**Table 2.**  
Assessment of resistance of selected buildings according to the modified point method

		Identification of the characteristics	Number of points
1.	Building length (m)	up to 15 m	4
2.	The shape of the solid	simple building plan, compact solid	0
3.	Foundation of the building	at a constant level	0
4.	Building subsoil	non-rocky soil with the exception of stony soil	0
5.	Building structure	brick strip foundation	3
		basement walls: brick masonry	1
		the lowest storey ceiling: arched ceiling on I-beams at $f/L < 1/10$	4
		lintels: brick flat	2
6.	Existing protection against mining influence	no protection	15
7.	Technical condition of the building <sup>1</sup>	natural wear of building: medium	2
		building damage: cracks up to 15 mm and inclination < 25 mm/m	8
Total points			39

<sup>1</sup> The assessment of the degree of natural wear of the building is currently performed before the next exploited seams start.

**Table 3.**  
Resistance of buildings to the influence of ground deformation – building qualification category according to the modified point method

Sum of points $n$ (-)	Permissible horizontal strain of the subsoil $\varepsilon_p$ (mm/m)	Building resistance category
$\leq 20$	7.0 – 9.0	4
21 – 23 24 – 29 30 – 33	6.0 5.0 4.0	3
34 – 36 37 – 43 44 – 46	3.0 2.5 2.0	2
47 – 49 50 – 56 57 – 59	1.5 1.0 0.5	1
$\geq 60$	$\leq 0.3$	0

### 3.2. Design conditions

#### 3.2.1. Analysis of the impact of exploitation on the building and determination of the resistance category of the object

The building is a typical single-family residential building in Upper Silesia, built in the second half of the 20<sup>th</sup> century. The building has two residential floors without an attic and a full basement. It has a masonry wall structure and is made of bricks with lime mortar, set on a clinker brick foundation. The ceiling over the basement is made as a sectional arched ceiling on steel I-beams. The upper ceiling and the hipped flat roof of the building are made of wood. This information, and the site inspection, made it possible to assess the building's resistance based on the point method, which was developed at the Central Mining Institute and is presented, among others, in [13]. The results of this assessment are presented in Table 2.

The assessment of the ability to accommodate the influences is made on the basis of the ranges given in Table 3.

The assigned range, together with the resistance category, determines the transferable values of the predicted ground deformation, which are given in Table 4. For the example of the building of interest, the resistance category 2 was assigned with the transferable horizontal strain of the ground being  $\varepsilon_p < 2.5$  mm/m.

#### 3.2.2. Stated effects of mining exploitation on the area in the vicinity of the building

In this area, mining operations have been carried out many times. The mine exploited nine seams, each of which influenced the object. The last exploitation ended in August 2009 and, by the end of the year, subsidence had terminated. Continuous deformations were included in the analysis from 1999 and, during this period, the object settled by a total of  $w = 1412$  mm, suffered permanent horizontal extension strain (with a value of  $\varepsilon = + 1.58$  mm/m) and temporarily experienced a contraction strain, with a peak value of  $\varepsilon = -3.19$  mm/m. There was also a peak slope of the terrain  $T = 4.51$  mm/m, which stabilised at  $T = 4.12$  mm/m. These values classify the area as deformation category II (Table 4) and, in the short term, category III, due to the peak negative values of the horizontal strain. In accordance with the adopted Regulation of the Minister of the Environment [19] on mining plant operation plans, it was allowed to exceed the ground deformation by one level, in

**Table 4.**  
Categories of mining area deformation [13]

Categories of mining area	The values of terrain deformation indicators		
	Inclination $T$ (mm/m)	Radius of curvature $R$ (km)	Horizontal strain $\varepsilon$ (mm/m)
0	$T < 0.5$	$ R  > 40$	$ \varepsilon  < 0.3$
I	$0.5 \leq T < 2.5$	$40 \geq  R  > 20$	$0.3 \leq  \varepsilon  < 1.5$
II	$2.5 \leq T < 5.0$	$20 \geq  R  > 12$	$1.5 \leq  \varepsilon  < 3.0$
III	$5.0 \leq T < 10.0$	$12 \geq  R  > 6$	$3.0 \leq  \varepsilon  < 6.0$
IV	$10.0 \leq T < 15.0$	$6 \geq  R  > 4$	$6.0 \leq  \varepsilon  < 9.0$
V	$T \geq 15.0$	$ R  \leq 4$	$ \varepsilon  \geq 9.0$

relation to building resistance, which was the case here.

Mining tremors appear with the occurrence of continuous deformations. They have a significant impact on the technical condition and construction of buildings. For the mining areas in the USCB, a scale of shock intensity for building structures was developed (GSIS-2017) [15]. In the period from April 2018 to February 2020, the mine's seismic stations registered

124 tremors. Taking into account the effects of damping or amplification vibrations in the ground over the distance between the hypocentre of the shock and the location of the building, the energy of the shock should not exceed  $E=2 \cdot 10^7$  J. Using the dependence of the ground surface given in [15], it is possible to estimate  $PGA_{H10}$  (Peak Ground Acceleration in horizontal direction for frequency up to 10 Hz) and  $PGV_{Hmax}$  (Peak Ground Velocity, maximal in horizontal direction) values, respective to  $200 \text{ mm/s}^2$  and  $5 \text{ mm/s}$ , which allows classification of the maximum shocks to the I degree of intensity (according to GSIS-2017). Despite the fact that the period of continuous deformations is earlier than the tremors considered, the influences of these deformations accumulate in the structure (inclination of the building, cracks caused by horizontal strain, etc.). In this case, shocks can cause more damage in contrast to undamaged buildings.

However, it should be mentioned that the geological situation in the area of the object is complex. The building is located on the other side of a geological fault, relative to the location of the mine and measurement stand. Measurements performed for a different object, but located on the same side of the fault, allowed us to see that, in some cases, there may



**Figure 6.**  
General view of the southern wall of the building



**Table 5.**  
Shock cases recorded on the measurement stand and estimated values in the mining forecast

Date	E (J)	PGA meas. (mm/s <sup>2</sup> )	PGA est. (mm/s <sup>2</sup> )	$t_{Ha}$ (s)	PGA meas./PGA est. (-)
18.04.2015	4.00E+09	258	230	3.90	1.1
05.08.2016	4.00E+06	459	151	1.54	3.0
02.01.2017	8.00E+06	629	142	1.66	4.4
27.01.2017	8.00E+06	300	143	1.55	2.1
21.02.2017	2.00E+06	313	95	1.78	3.3
14.03.2017	2.00E+06	310	121	1.72	2.6



**Figure 7.**  
Cracking of the walls and ceilings inside the building



**Figure 8.**  
Cracking of the entrance stairs and the splash apron around the building

be an increase in the value of the shock acceleration in relation to the forecast calculations. For six comparative analyses, it was found that the amplification of shock acceleration in relation to the estimated values reached up to 4.4 times (Table 5).

The large disparity between the measured and estimated values may be due to the presence of a fault

that disturbs the transmission of the shock. The first shock in Table 5 has also been taken into consideration, although it is outside the applicability of Eq. (3), but there is no other approximation for this phenomenon in this region.

Such levels of measured acceleration make it possible to classify the shocks to the II degree of intensity, which clearly increases the negative impact on the object. In this case, the following effects can be expected in the facility:

- elongation of cracks,
- falling off of small fragments of detached internal and external plaster,
- loosening of poorly fixed ceramic tiles,
- falling off of fragments of damaged cornices and poorly fastened pinnacles,
- more intense brick loosening in brick chimneys,
- more intense loosening of tiles, including sliding,
- intensification of cracks at the joints of structural elements (e.g. wall-ceilings in prefabricated buildings), especially those made of different construction materials, and
- the intensification of cracks at the joints of faulty plasterboard surfaces.

### 3.2.3. Damage to the building

A general view of an external wall of the building is shown in Fig. 6. As a result of an inspection of the building, the following damage was found:

- cracking of the external walls of the building,
- cracking of the walls and ceilings inside the building (Fig. 7),
- the slope of the floor is strongly felt, and
- cracking of the splash apron around the building and the entrance stairs (Fig. 8).

Apron failures are partly due to material or workmanship defects, but they are intensified by horizontal strain and ground settlement.

The causes of building damage were both continuous deformation and ground shocks. Continuous deformation of the ground caused damage in the form of cracking of the concrete splash apron around the building and cracks in the entrance stairs to the building, which were caused by the occurrence of horizontal strain and differential settlement. These cracks were up to 5 mm. The slope of the terrain determined in the ground deformation forecasts was set at over 4‰, but it was felt in the building. The inclination of

buildings is usually greater than the slope of the terrain, which results from the redistribution of stresses in the ground under the foundation of the inclined object and their concentration under the lowered edge of the building, as presented in [21]. According to the adopted scale of inconvenience of the building inclination [6], an inclination of up to 10‰ is imperceptible to users. Therefore, it should be assumed that the building is placed in the second part of this range of the scale. The cracks appearing inside the building were caused by the static effects of the continuous deformation of the ground and ground shocks. Repeated shocks intensified cracks in the finishing elements of the facility (interior plaster and cladding) but may have also caused structural cracking. New cracks in the building, which appeared after the shocks, were reported to the mine services for their registration and subsequent removal. Fig. 7 shows cracks at the joints of walls and ceilings, which occur both in the finishes and the structural elements.

#### 4. CONCLUSIONS

Intensive underground mining of coal in Upper Silesia is largely carried out beneath urbanised areas. Filling of the post-mining voids with the rock layers located above them causes the onset of ground deformation, which has a significant impact on objects on the ground surface. Depending on the intensity of the ground deformation and the technical condition of the objects, the damage to them varies from minor cracks to damages that preclude further use.

A significant number of buildings affected by mining operations require a simple method of assessing their damage. The modified point method offers such possibilities but, due to the large number of assessed objects, it is, inevitably, not very detailed and is limited to the assessment of the effects of continuous ground deformations. We showed this by using an example of a simple residential building.

The use of the point method, as a criterion for classifying an object into an appropriate resistance group, is not fully justified in the case of ground shocks accompanying the disclosure of deformations. The presented example, of a building exposed to the simultaneous action of significant continuous deformations and ground shocks, shows that the repeated impact of shocks causes increasing damage to the building. This is the reason for lowering the resistance category of an object which, in turn, increases the costs incurred for repairing damage.

It would be necessary to take into account the impact of ground shocks in the point method of building resistance. As part of the point method, a parameter should be introduced that takes into account the occurrence of shocks, both in terms of the size and the number of shocks that occurred in previous periods of exploitation. However, the situation is difficult because of the magnitude of the energy emitted by the ground shocks, which are phenomena caused by exploitation and cannot be fully controlled.

#### REFERENCES

- [1] Bian Z.F., Miao X.X., Lei S.G. (2012). The challenges of reusing mining and mineral-process in wastes. *Science*, 337(6095), 702–703.
- [2] Chudek M. (2010). *Mechanika górotworu z podstawami zarządzania ochroną środowiska w obszarach górniczych i pogórnich* (Rock mass mechanics with the basics of environmental protection management in mining and post-mining areas). Wydawnictwo Politechniki Śląskiej.
- [3] Deck O., Al Heib M., Homand F. (2003). Taking the soil–structure interaction into account in assessing the loading of a structure in a mining subsidence area. *Engineering Structures*, 25(4), 435–448. Retrieved from [https://doi.org/10.1016/S0141-0296\(02\)00184-0](https://doi.org/10.1016/S0141-0296(02)00184-0).
- [4] Eugênio T.M.C., Fagundes J.F., Viana Q.S., Vilela A.P., Mendes R.F. (2021). Study on the feasibility of using iron ore tailing (iot) on technological properties of concrete roof tiles. *Construction and Building Materials*, 279, 1–19. Retrieved from <https://doi.org/10.1016/j.conbuildmat.2021.122484>.
- [5] Florkowska L. (2013). Example building damage caused by mining exploitation in disturbed rock mass. *Studia Geotechnica et Mechanica*, 35(2), 19–38.
- [6] Instrukcja GIG 12/2000. (2000). *Zasady oceny możliwości prowadzenia podziemnej eksploatacji górniczej z uwagi na ochronę obiektów budowlanych* (Principles of assessing the possibility of conducting underground mining due to the protection of buildings). Wydawnictwo Głównego Instytutu Górnictwa.
- [7] Instrukcja ITB nr 416/2006. (2006). *Projektowanie budynków na terenach górniczych* (Designing buildings in mining areas). Wydawnictwo ITB.
- [8] Kapusta Ł., Szojda L. (2021). The role of expansion joints for traditional buildings affected by the curvature of the mining area. *Engineering Failure Analysis*, 128, 1–25. Retrieved from <https://doi.org/10.1016/j.engfailanal.2021.105598>.
- [9] Karácsonyi B. (1979). Guiding principles for the preparation of hydrological maps for building. *Bulletin of the International Association of Engineering Geology*, 19, 237–241. Retrieved from <https://doi.org/10.1007/BF02600481>.

- [10] Knothe S. (1984). Prognozowanie wpływów eksploatacji górniczej (Forecasting the influences of mining exploitation). Wydawnictwo Naukowe “Śląsk”.
- [11] Kratzsch H. (1983). Mining Subsidence Engineering. Springer-Verlag.
- [12] Kwiatek J. (2002). Obiekty budowlane na terenach górniczych (Building structures in mining areas). Wydawnictwo Głównego Instytutu Górnictwa.
- [13] Kwiatek J. et al. (1997). Ochrona obiektów budowlanych na terenach górniczych (Protection of buildings in mining areas). Wydawnictwo Głównego Instytutu Górnictwa.
- [14] Marescotti P., Azzali E., Servida D. (2010). Mineralogical and geochemical spatial analyses of a waste-rock dump at the Libiola Fe–Cu sulphide mine (Eastern Liguria, Italy). *Environmental Earth Sciences*, 61, 187–199. Retrieved from <https://doi.org/10.1007/s12665-009-0335-7>.
- [15] Mutke G. i inni (2018). Zasady stosowania Górnictwa Skali Intensywności Sejsmicznej GSIS-2017 do prognozy i oceny skutków oddziaływania wstrząsów indukowanych eksploatacją na obiekty budowlane oraz klasyfikacji ich odporności dynamicznej (Principles of applying the Mining Seismic Intensity Scale GSIS-2017 to the forecast and assessment of the effects of shocks induced by exploitation on building structures and the classification of their dynamic resistance). *Prace Naukowe GIG, Górnictwo i Środowisko*, 64.
- [16] Orwat J. (2020). Mining exploitation forecasted effects caused by a hard coal extraction from a thick seam. *Journal of Physics: Conference Series*, 1426(1), 1–8.
- [17] Orwat J., Gromysz K. (2021). Occurrence consequences of mining terrain surface discontinuous linear deformations in a residential building. *Journal of Physics: Conference Series*, 1781(1), 1–11.
- [18] Quanyuan W., Jiewu P., Shanzhong Q., Yiping L., Congcong H., Tingxiang L., Lime H. (2009). Impacts of coal mining subsidence on the surface landscape in Longkou City, Shandong Province of China. *Environmental Earth Sciences*, 59, 783–791.
- [19] Rozporządzenie Ministra Środowiska z dnia 8 grudnia 2017 r. w sprawie planów ruchów zakładów górniczych (Regulation of the Minister of the Environment of December 8, 2017 on mining plant operations plans). *Dziennik Ustaw z 2017 poz. 2293*.
- [20] Saeidi A., Deck O., Verdel T. (2009). Development of building vulnerability functions in subsidence regions from empirical methods. *Engineering Structures*, 31(10), 2275–2286. Retrieved from <https://doi.org/10.1016/j.engstruct.2009.04.010>.
- [21] Słowik L. (2015). Wpływ nachylenia terenu spowodowanego podziemną eksploatacją górniczą na wychylenie obiektów budowlanych (The influence of the slope of the terrain caused by underground mining on the inclination of buildings) (PhD thesis, Building Research Institute), Poland, Warszawa.
- [22] Stockmann M., Hirsch D., Lippmann-Pipke J. (2013). Geochemical study of different-aged mining dump materials in the Freiberg mining district, Germany. *Environmental Earth Sciences*, 68, 1153–1168. Retrieved from <https://doi.org/10.1007/s12665-012-1817-6>.
- [23] Strzałkowski P. (2019). Some remarks on impact of mining based on an example of building deformation and damage caused by mining in conditions of Upper Silesian Coal Basin. *Pure and Applied Geophysics*, 176(6), 2595–2605.
- [24] Strzałkowski P. (2015). Zarys ochrony terenów górniczych (Outline of the protection of mining areas). Wydawnictwo Politechniki Śląskiej.
- [25] Szojda L., Kapusta Ł. (2021). Numerical analysis of the influence of mining ground deformation on the structure of a masonry residential building. *Archives of Civil Engineering*, 67(3), 243–257.
- [26] Szojda L., Wandzik G. (2019). Discontinuous terrain deformation – forecasting and consequences of their occurrence for building structures. 29th International Conference on Structural Failures. ICSF 2019, 1–12. Retrieved from <https://doi.org/10.1051/mateconf/201928403010>.
- [27] Ścigała R. (2008). Komputerowe wspomaganie prognozowania deformacji górotworu i powierzchni wywołanych podziemną eksploatacją górniczą (Computer aided forecasting of rock mass and surface deformations caused by underground mining). Wydawnictwo Politechniki Śląskiej.
- [28] Ustawa z dnia 9 czerwca 2011 r. Prawo geologiczne i górnicze (The Act of June 9, 2011 Geological and Mining Law). *Dziennik Ustaw z 2011 nr 163 poz. 981 z późn. zm.*
- [29] Vandana M., John S.E., Maya K. (2020). Environmental impact of quarrying of building stones and laterite blocks: a comparative study of two river basins in Southern Western Ghats, India. *Environmental Earth Sciences*, 79(14), 1–15. Retrieved from <https://doi.org/10.1007/s12665-020-09104-1>.
- [30] Whittaker B.N., Reddish, D.J. (1989). Subsidence Occurrence, Prediction and Control. Developments in Geotechnical Engineering. Elsevier.
- [31] Zhu X., Guo G., Zha J., Chen T., Fang Q., Yang X. (2016). Surface dynamic subsidence prediction model of solid backfill mining. *Environmental Earth Sciences*, 75(12), 1–9.